Sonochemical synthesis, characterization, and effects of temperature, power ultrasound and reaction time on the morphological properties of two new nanostructured Mercury(II) coordination supramolecule compounds

Payam Hayati [a], Ali Reza Rezvani [a*], Ali Morsali [b*], Daniel Ruiz Molina[c*], Samira Geravand[a], Salvio Suarez-Garcia[c], Miguel Angel Moreno Villaecija[c], S.García-Granda[e], Rafael Mendoza-Meroño[e], Pascal Retailleau[d]

[a] Department of Chemistry, Faculty of Sciences, University of Sistan and Baluchestan, P.O. Box 98135-674, Zahedan, Iran.

[b] Department of Chemistry, Faculty of Sciences, Tarbiat Modares University, P.O. Box 14115-4838, Tehran, Islamic Republic of Iran.

[c] Catalan Institute of Nanoscience and Nanotechnology (ICN2), CSIC and The Barcelona Institute of Science and Technology, Campus UAB, Bellaterra 08193, Barcelona, Spain.

[d] Institut de Chimie des Substances Naturelles, CNRS UPR 2301, Univ. Paris-Sud, Université Paris-Saclay, 1, av. de la Terrasse, 91198 Gif-sur-Yvette, France.

[e] Departamento de Química Física y Analítica, Universidad de Oviedo, 33006 Oviedo-CINN, Spain.

Abstract

Two new mercury(II) coordination supramolecular compounds (CSCs) (1D and 0D), $[Hg(L)(I)_2]_n$ **(1)** and $[Hg_2(L^{/})_2(SCN)_2].2H_2O$ **(2)** (L= 2-amino-4-methylpyridine and $L^{/}$= 2,6-pyridinedicarboxlic acid), have been synthesized under different experimental conditions. Micrometric crystals (bulk) or nano-sized materials have been obtained depending on using the branch tube method or sonochemical irradiation. All materials have been characterized by field emission scanning electron microscope (FESEM), scanning electron microscopy (SEM), powder X-ray diffraction (PXRD) and FT-IR spectroscopy. Single crystal X-ray analyses on compounds **1** and **2** show that Hg^{2+} ions are 4-coordinated and 5-coordinated, respectively. Topological analysis shows that the compound **1** and **2** have 2C1, **sql** net. The thermal stability of compounds

1 and **2** in bulk and nano-size has been studied by thermal gravimetric (TG), differential thermal analyses (DTA) and differential scanning calorimetry (DSC). Also, by changing counter ions were obtained various structures **1** and **2** (1D and 0D, respectively). The role of different parameters like power of ultrasound irradiation, reaction time and temperature on the growth and morphology of the nano-structures are studied. Results suggest that increasing power ultrasound irradiation and temperature together with reducing reaction time and concentration of initial reagents leads to a decrease in particle size.

Keywords: Coordination supramolecular, Sonochemical process, Ultrasound irradiation, Morphology.

Introduction:

In recent years, the design and synthesis of CSCs have drew more and more attention not only due to their tremendous potential applications in molecular recognition [1], nonlinear optics [2], magnetism [3], metal ion selection [4], heterogeneous catalysis [5], and gas storage [6], but also for their intriguing structural diversity and interesting hydrogen bonding network [7-8]. Generally, the kind of metal ions, the selection of auxiliary ligand, geometry and number of coordination sites provided by organic ligands are all important parameters in the self-assembly processes of CSCs. Among these parameters, the selection of organic ligand with suitable binding groups is especially crucial [9-16].

Mercury(II) is a well-known metal with a wide range of applications in different areas. However, mercury has not been used widely for the fabrication of coordination polymers in the literature [15–22]. The d^{10} configuration of the Hg(II) ion is associated with a flexible coordination environment so that different geometries can be generated to tailor-make materials [18]. The

CSCs of this metal ion can be synthesized through different methods, such as the diffusion-based method, layering technique, evaporation route, hydrothermal synthesis, crystallization technique and ultrasonic irradiation method [23-29].

Sonochemical synthesis of various types of nanoparticles and nanostructured materials composed of noble metals [30-32], transition metals [33-34], semiconductors [36], carbon materials [37], and polymeric materials [38], have received much attention in recent years. This is due to the unique reaction routes induced by acoustic cavitation in solution, which provides extreme conditions of transient high temperature and high pressure within the collapsing bubbles, shock wave generation, and radical formation [39 and 65-67].

Nanostructured materials have been intensively studied in recent years because the physical properties of these materials are often quite different from those of the bulk [40-43]. Nano size CSCs are attractive to explore, since controlling the growth of materials at the sub-micrometer scale is of the central importance in the emerging field of nanotechnology [44]. CSCs with various morphologies, e.g., nanospheres, nanocubes, nanosheets, and nanorods have been prepared by various synthetic techniques, such as precipitation, microemulsion, and solvothermal techniques, as well as microwave-assisted methods [45-46]. The development of mild, green, low-cost, large-scale, environmentally responsible, and more flexible methods for creating controllable morphologies of nano/microstructures CSCs are strongly desired [47,48].

The effects of ultrasound radiation on chemical reactions were reported in the recent works [50-52]. In this manuscript, we have developed a simple sonochemical to prepare nano-structures of $[Hg(L)(I)_2]_n$ **(1)** and $[Hg_2(L')_2(SCN)_2].2H_2O$ **(2)**. The power of ultrasound irradiation, sonicating time, temperature of reaction, and concentration of initial reactants were the parameters which were evaluated for reaching the optimized condition. Scanning electron

microscopy (SEM) and powder X-ray diffraction (PXRD) were used for the characterization of the products. In addition, we have investigated the influence of additives on the particle size and particle size distribution. These were achieved by employing a sonochemical method, and using different additives to control the particle size and the particle size distribution.

2. Experimental

2.1. Materials and physical techniques

Starting reagents for the synthesis were purchased and used without any purification from industrial suppliers (Sigma–Aldrich, Merck and others). Elemental analyses (carbon, hydrogen, and nitrogen) were performed employing a Heraeus Analytical Jena, Multi EA 3100 CHNO rapid analyzer. Fourier transform infrared spectra were recorded on a FT-IR JASCO 680-PLUS spectrometer as KBr pellets in the 4000–400 cm^{-1} spectral range, also infrared spectra (IR) were obtained using the instrument Bruker Tensor 27 FT-IR with a single window reflection of diamond ATR (Attenuated total reflectance) model MKII Golden Gate, Specac and the OPUS data collection programme software. The instrument is equipped with a room temperature detector, and a mid-IR source (4000 to 400 cm^{-1}). Since it is a single beam instrument, it was needed to run a background spectrum in air before the measurement.

Thermal gravimetric analysis (TGA), differential thermal analyses (DTA) and differential scanning calorimetry (DSC) of the title compound were performed on a computer-controlled STA - PT 1500 apparatus, also thermal measurements were performed with PerkinElmer Pyris instrument by using platinum pans. The curves were recorded in temperature range from 30°C to 650°C at 10ºC/min under nitrogen atmosphere with flow rate 60 mL/min. The data obtained was processed with Pyris and Opus software and calorimetry measurements were done by

PerkinElmer 8000 equipment by using aluminium pans under nitrogen atmosphere in the temperature range between 10-400°C. Single phase powder sample of 1 - 1, 2 – 1, 3 – 1 and 4 – 1 crystal structure compound **1** and **2** were loaded into alumina pans and heated with a ramp rate of 10 °C/min from room temperature to 650 °C under argon atmosphere. Single crystal X-ray diffraction experiments were carried out for compounds **1** and **2** with MoKα radiation (λ=0.71073 Å) at ambient temperature. A microfocused Rigaku mm003 source with integrated confocal caxFlux double bounce optic and HPAD Pilatus 200K detector were used for **1** and **2** while for 2 data were measured on a Bruker-Nonius Kappa CCD diffractometer, also Powder X-ray diffraction patterns were recorded on PANalytical X'Pert PRO MRD diffractometer equipped with a Cu Kα radiation source (λ = 1.54184 Å). The structures were solved by direct methods and refined by full matrix least squares on F^2. All non-hydrogen atoms were refined anisotropically. Hydrogen atoms were included in structure factor calculations from their location in difference maps. C-bound H atoms were treated as riding in geometrically idealized positions, with Uiso (H) = kUeq (C), where k = 1.2 for the Csp^2 - bound H atoms. For the water molecules, the oxygen-hydrogen bond lengths were restrained to 0.82(2) Å (DFIX instruction) and the hydrogen-hydrogen intramolecular distances were restrained to 1.30(4) Å (DANG instruction). The U_{iso} value for hydrogen atoms were set to 1.5 times the value of the water oxygen atom. Computing details: data collection, cell refinement and data reduction: CrystalClear-SM expert 2.1b43 [53]; program(s) used to solve structure: SHELXT [54]; program(s) used to refine structure: SHELXL-2014/7 [54]; molecular graphics: PLATON [55]; reduction of data and semiempirical absorption correction: SADABS program[56]; direct methods (SIR97 program[57]); full-matrix least-squares method on F^2: SHELXL-97 program [58] with the aid of the program WinGX [59]. X-ray powder diffraction (XRD) measurements

were performed using an X'pert diffractometer manufactured by Philips with monochromatized Cuka radiation and simulated XRD powder patterns based on single crystal data were prepared using the Mercury software [60]. The samples were characterized with a scanning electron microscope (SEM) (Philips XL 30 and S-4160), Images obtained from SEM measurements were performed on a scanning electron microscope (FEI Quanta 650 FEG) in mode operation of secondary electrons (SE) with a beam voltage between 15 and 20 KV. The samples were prepared by deposition of a drop of the material previously dispersed properly solvents on aluminium stubs followed by evaporation of the solvent under ambient conditions. Before performing the analysis, the samples were metalized by depositing on the surface a thin platinum layer (5 nm) using a sputter coater (Leica EM ACE600), and field emission scanning electron microscope (FE-SEM) (Perkin Elmer Elan 9000) with gold coating. A multi wave ultrasonic generator (ultrasonic homogenizer-UP 400-A, IRAN) and Elmasonic (Elma) S40 H, equipped with a converter/transducer and titanium oscillator (horn), 12.5 mm in diameter, operating at 20 kHz with a maximum power output of 400 W, were used for the ultrasonic irradiation. Melting points were measured on an electrothermal 9100 apparatus and are uncorrected.

2.4. Synthesis of $[Hg(L)(I)_2]_n$ (1) as single crystal

$HgCl_2$ (1 mmol, 0.271 g), 2-Amino-4-methylpyridine (1 mmol, 0.108 g) and potassium iodide (2 mmol, 0.332 g) were loaded into one arm of a branch tube and both of the arms were filled slowly by water. The chemical bearing arm was immersed in an oil bath kept at 60 °C. crystals were formed on the inside surface of the arm kept at ambient temperature after, After15 days, colorless crystals were deposited in the cooler arm were filtered off, washed with water and air

dried. (0.164g, yield 29.18% based on final product **1**), m.p. = 155 °C. Anal. Calc. for $C_6H_8HgI_2N_2$: C: 12.79, H: 1.42, N: 4.97%; Found C: 12.74 H: 1.39 N: 4.96 %. IR (selected bands for compound **1**; in cm^{-1}): 3439.88(s), 3325.51 (s), 3022.60 (w), 1624.55(s), 1450.56(s) cm^{-1}.

2.5. Synthesis of $[Hg(L)(I)_2]_n$ (1) nano-structures under ultrasonic irradiation

To prepare the nano-structures of $[Hg(L)(I)_2]_n$ (**1**) by another sonochemical process, a high-density ultrasonic probe immersed directly into the solution of $HgCl_2$ (20 mL, 0.05 M) in water, then into this solution, a proper volume of 2-Amino-4-methylpyridine ligand and KI in water solvent (20 mL, 0.05 M) was added in a drop wise manner. The solution was ultrasonically irradiated with the power of 60W and temperature 50 °C for 1 h. For the study of the effect of time on size and morphology of nano- structured compound **1**, the above processes were done with 30 min and for the study of the effect of sonication power with 80W (time:1h, tempteture:50°C, concentration:0.05M) also for the study of the effect of temperature with 80°C(time:1h, sonication power: 60W, concentration:0.05M) has been done too. The obtained precipitates were filtered, subsequently washed with water and then dried. (0.248 g, yield 44.12% based on final product **1**), m.p. =172 °C. Anal. Calc. for $C_6H_8HgI_2N_2$: C: 12.79, H: 1.42, N: 4.97%; Found C: 12.77 H: 1.36 N: 4.94 %. IR (selected bands for compound **1**; in cm^{-1}): 3441.02(s), 3310.18(s), 3034.43(w), 1653.89(s), 1446.24(s) cm^{-1}.

2.6. Synthesis of $[Hg_2(L^{/})_2(SCN)_2].2H_2O$ (2) as single crystal

$HgCl_2$ (1 mmol, 0.271g), 2, 6-pyridinedicarboxlic acid (2 mmol, 0.334 g) and KSCN (1 mmol, 0.09) were loaded into one arm of a branch tube and both of the arms were filled slowly by

water. The chemical bearing arm was immersed in an oil bath kept at 60 °C. Crystals were formed on the inside surface of the arm kept at ambient temperature, After one week, colorless crystals were deposited in the cooler arm were filtered off, washed with water and air dried. (0.214 g, yield 49.08% based on final product), product **2** (single crystal): m.p. = 150 °C. Anal. Calc. for $C_{16}H_8Hg_2N_4O_8S_2.2H_2O$: C: 21.67, H: 0.90, N: 6.32%; Found C: 21.56 H: 0.89 N: 6.28 %. IR (selected bands for compound **2**; in cm^{-1}): 3434.26(br), 3095.74 (br), 2141.74(s), 2109.54(w), 1693.76 (s) cm^{-1}.

2.7. Synthesis of $[Hg_2(L^{/})_2(SCN)_2].2H_2O$ (2) nano-structures under ultrasonic irradiation

To prepare the nano-structures of $[Hg_2(L^{/})_2(SCN)_2].2H_2O$ (**2**) by sonochemical process, a high-density ultrasonic probe immersed directly into the solution of $HgCl_2$ (20 mL, 0.05 M) in water, then into this solution, a proper volume of 2, 6-pyridinedicarboxlic acid ligand and KBr in water solvent (20 mL, 0.05 M) was added in a drop wise manner. The solution was irradiated by sonochemical with the power of 60W and temperature 50 °C for 1 h. For the study of the effect of time of reaction on size and morphology of nano- structured compound **2**, the above processes were done with 30 min and for the study of the effect of sonication power with 80W (time: 1h, temperature: 50°C, concentration: 0.05M) also for the study of the effect of temperature with 80°C (time: 1h, sonication power: 60W, concentration: 0.05M) has been done too. The obtained precipitates were filtered, subsequently washed with water and then dried. (0.235 g, yield 53.89% based on final product), product **2** (nano-structure), m.p. =166 °C. Anal. Calc. for $C_{16}H_8Hg_2N_4O_8S_2.2H_2O$: C: 21.67, H: 0.90, N: 6.32%; Found C: 21.61 H: 0.88 N: 6.31 %. IR (selected bands for compound **2**; in cm^{-1}): 3433.83(br), 3093.32(br), 3035.55(w), 2132.65(s), 2101.32(w), 1691.21(s) cm^{-1}.

3. Results and discussion

Reaction between the organic nitrogen and oxygen-donor 2-amino-4-methylpyridine ligand (L) and $L^{/}$= 2,6-pyridinedicarboxlic acid, potassium iodide, potassium thiocyanate and mercury (II) chloride yielded crystalline material formulated as new 1D and 0D coordination supramolecular compounds $[Hg(L)(I)_2]_n$ (**1**) and $[Hg_2(L)_2(SCN)_2].2H_2O$ (**2**). Nanocrystals of compound **1** and **2** were obtained in aqueous solution by ultrasonic irradiation. Single crystals of compound **1** and **2**, suitable for X-ray crystallography, were prepared by thermal gradient method applied to an aqueous solution of the reagents the ‘‘branched tube method‘‘. $[Hg(L)(I)_2]_n$ (**1**) and $[Hg_2(L)_2(SCN)_2].2H_2O$ (**2**), synthesized by using the two different routes (branched tube and ultrasonic method). Single crystal X-ray diffraction analysis (Tables 1- 4) of compounds **1** and **2** were carried out and the coordination environment of the title complexes are shown in (Fig .1) Single X-ray crystal analysis reveals that $[Hg(L)(I)_2]_n$ (**1**) and $[Hg_2(L)_2(SCN)_2].2H_2O$ (**2**) complexes crystallize in monoclinic and monoclinic space group, P 21/c and P 21/c, respectively.

In compound **1**, also Hg(II) atoms are coordinated by four atoms and have distorted tetrahedral coordination sphere as I_3N (Fig. 1). Asymmetric unit cell of compound **2** consists of one Hg^{+2} cation, one 2-amino-4-methylpyridine ligand, and two I^- anions (Fig. 4). Each Hg atom is coordinated by nitrogen atom of 2-amino-4-methylpyridine ligand and two I^- anions with Hg–N, and Hg-I distances are about 2.317-2.999Å (Table 2 and Fig. 2). The coordination interactions can be separated in two groups: i) Relatively strong valence in range of 0.870-2.999 Å; ii) More weak electrostatic, in long range of 2.578-4.214 Å.

Both terminal and bridge I^- ions additionally interact with neighbor Hg^{2+} ion, but with much longer distances Hg(1)-I(1)=2.737 Å and Hg(1)-I(2)=2.657 Å.

Strong bonds form mononuclear complexes [Hg(L)(I)], which expanded by relatively weak interactions in polymeric chain $[Hg_2(L)(I)_2]_n$ along *a* axis (Fig. 2). Simplification of mononuclear complexes $[Hg(L)(Br)_2]$ into nodes of the chain underlying net and its classification by ToposPro package reveals 2C1 topological type, which is abundant for 1D CPs [(more than 45000 examples in TTO collection of ToposPro (Fig. 5)] [61]. Every [Hg(L)(I)] chain is surrounded by eight other same chains forming van-der-waals bonded hexagonal packing of cylinders (Fig. 2).

The Hg(II) atoms of compound **2** are coordinated by two N, O and one S atoms and composing square pyramid coordination N_2O_2S (Fig. 1). The asymmetric unit of compound **2** contains two Hg^{2+} cations, which is coordinated with two 2,6-pyridinedicarboxlic acid ligand and two SCN^- anions (Fig. 4). Each 2,6-pyridinedicarboxlic acid ligand in compound **2** is coordinated to one Hg atom by N and O atoms, and Hg-N and Hg-O distance are about 2.41 and 2.46 Å, respectively. Additionally, two N and S atoms are coordinated to each Hg (II) atom with contacts distances Hg–N and Hg-S in the range of 2.37-2.41 Å (Table 3 and Fig. 3). Two of SCN^- anions are bridging between two Hg^{2+} cations, and two SCN^- are terminal occupying one vertex of base in trigonal pyramidal coordination polyhedron of each Hg^{2+}. The coordination interactions can be separated in two groups:

i) Strong, more valence, in short range of 2.217-2.528 Å;

ii) Weak, more electrostatic, in long range of 3.021-3.628 Å.

Both bridge SCN^- ions additionally interact with neighbor Hg^{2+} ion, but with much longer distances Hg(1)A-N(1)A=2.217(3) Å and Hg(1)B-N(2)B=2.419 Å.

Simplification of mononuclear complexes $[Hg_2(L)_2(SCN)_2].2H_2O$ into nodes underlying net and its classification by ToposPro package reveals **sql** topological type, which is abundant for 1D coordination polymers (more than 1700 examples in TTO collection of ToposPro (Fig. 5). Every $[Hg_2(L)_2(SCN)_2].2H_2O$ molecule is surrounded by six other same molecules forming van-der-waals bonded hexagonal packing (Fig. 3).

The IR spectra display characteristic absorption bands for N-H, C-H and the 2-amino-4-methylpyridine ligand in compound **1**. The IR spectrum of compound **1** shows two bands around 3454 and 3359 cm^{-1} are due to the N-H stretching frequency amine group ligand. The absorption bands with variable intensity in the frequency range 1640–1560 cm^{-1} correspond to N-H bending frequency of the amine group of the 2-amino-4-methylpyridine ligand, absorption bands around 1454 cm^{-1} related to CH_3 bending. Also, aromatic C-H stretching frequency appears at around 3035 cm^{-1}. The elemental analysis and IR spectra of the nano-structure produced by the sonochemical method as well as the bulk material produced by the branched tube method are indistinguishable (Fig. 6). Also, The IR spectra show characteristic absorption bands for 2, 6-pyridinedicarboxlic acid ligands in compound **2**. The IR spectrum of compounds **2** show the characteristic stretching frequency of O-H group observed at about 3442 cm^{-1} the relatively broad absorption bands, The absorption bands with variable intensity in the frequency range 1700–1750 cm^{-1} correspond to C=O stretching frequency from the carbonyl of the 2,6-pyridinedicarboxlic acid ligands. Also, characteristic band of the C-O stretching frequency carboxylic acid group appears at 1000-1300 cm^{-1}. The absorption bands around 2141 and 2109 cm^{-1} related to stretching frequency of the SCN group. Also, aromatic C-H stretching frequency appears at around 3035 cm^{-1}. The elemental analysis and IR spectra of the nano-structure

produced by the sonochemical method as well as the bulk material produced by the branched tube method are indistinguishable (Fig. 6).

Figure. 7 shows the XRD patterns of compounds **1** and **2** simulated from single crystal X-ray data. While the experimental XRD patterns of compounds **1** and **2** prepared by the sonochemical process is shown in Figure. 7. For **1** and **2** compounds, acceptable matches, with slight differences in 2θ, were observed between the simulated and experimental powder X-ray diffraction patterns. This indicates that the compound **1** and **2** obtained by the sonochemical process as nano-structures are identical to that obtained by single crystal diffraction. The significant broadening of the peaks indicates that the particles are of nanometer dimensions. Figure. 7 shows if the pick is sharper, then crystal lattice will be more regular. Also, for crystal and nano structures compound **1** and **2** are concluded which have same phase.

In order to look at the thermal stability of the four compounds, thermal gravimetric (TG), differential thermal analyses (DTA) and differential scanning calorimetry (DSC) were carried out for compounds **1** and **2** between 30 and 650°C under nitrogen flow.

The TG curve of compound **1** indicates that this compound is stable up to 110 °C, at which temperature it begins to decompose (Fig. 8). DTA curve in figure 8 shows two exothermic at 220 and 325°C, also removal of the 2-amino-4-methylpyridine ligand connected to Hg atom ligand occur in one steps between 120 and 280 °C, with a mass loss 98.28%. Mass loss calculations show that the final decomposition product is HgI_2 (Fig. 8).

The TG curve of compound **2** indicates that the compound does melt and is stable up to 50 °C at that temperature it begins to decompose (Fig. 8). A first weight loss over 50–100 °C

corresponding to the loss of coordinated and lattice water molecules with one endothermic peak. Pyridine aromatic ring and two carboxylate groups of 2,6-pyridinedicarboxlic acid ligand carry out in range of 110 to 420 °C, respectively. DSC curve in figure 8 shows decomposition of the aromatic rings of pyridine aromatic ring and two carboxylate groups of 2,6-pyridinedicarboxlic acid ligand takes place in three steps with one exothermic between from 100 to 180 °C , 380 to 420 °C and 420 to 490 °C with one exothermic , one exothermic and two exothermic ,two endothermic, with a mass loss of 10.25%, 52.26 % and 17.12 % respectively. Mass loss calculations show that the final decomposition product is HgO (Fig. 8).

Various conditions for preparation of compounds **1** and **2** nano-structures were summarized in Table 4. In this table, sample 1 – 1 and 2 – 1 were studied without power ultrasound and the other samples were studied under variable temperature, time and power ultrasound. In order to research the role of power ultrasound irradiation on the character of product, reactions were performed under completely different power ultrasound irradiation. Results show a decrease in the particles size as increasing power ultrasound irradiation [62-64].

In sample 1 - 1, the reactions were studied without power ultrasound. Results show that size particles sample of 1 - 1 (Fig. 9a) is larger than 1 - 2 (Fig. 9b), these results are similar with samples 2 – 1, 2 – 2 (Fig. 10a, b). Table 4, shows the average diameter field emission scanning electron microscope (FESEM) and scanning electron micrographs (SEM) of the prepared samples. Results show high power ultrasound irradiation decreased agglomeration, and thus led to decrease particles size. Comparison between samples 1 - 2 and 1 - 3 shows a decrease in nanoparticle size. Thus, size particles of sample 1 - 3 are smaller than 1 – 2 (Fig. 9b, c). These facts are repeated in samples 2 – 2, 2 – 3 (Fig. 10b, c). However, a reducing the reaction time led

to the decrease of size particles. Particle sizes and morphology of nanoparticle are depending on temperature [62]. Higher temperature (70 °C) results in an increased solubility, and thus a reduced supersaturation of growth species in the solution, and thus particles size of sample 1 - 4 is smaller than particles size of sample 1 – 2 (Fig. 9d, b). These facts are repeated in samples 2 – 4, 2 – 2 (Fig.10d, b). Table 6, shows the average diameter of particles shown by field emission scanning electron microscope (FESEM) and scanning electron micrographs (SEM) of the prepared samples. Pay attention to, the best conditions for getting a small sized and less agglomerated nanostructure materials for these four mercury coordination supramolecular compounds are temperature, reaction time and the power of ultrasonic irradiation 70 ºC, 60 min and 60 W, respectively. Also, other condition (temperature =50 ºC, reaction time= 30min and power of ultrasonic irradiation=60W) is good for obtaining small nanoparticle size.

4. Conclusion

Two new Hg(II) coordination supramolecular compounds $[Hg(L)(I)_2]_n$ (**1**) and $[Hg_2(L^{/})_2(SCN)_2].2H_2O$ (**2**), (L= 2-amino-4-methylpyridine and $L^{/}$= 2,6-pyridinedicarboxlic acid), have been synthesized utilizing a thermal gradient approach and also by sonochemical irradiation. Compounds **1** and **2** were structurally characterized by means of single crystal X-ray diffraction. The crystal structures of compounds **1** and **2** are made up of 1D and 0D CSCs and show the relevant coordination number for the Hg(II) ions are four and five. Topological analysis shows that the compound 1 and 2 have 2C1, **sql** net. In summary, we can obtain the new Hg(II) CSCs with change to counter ion and initial concentration of reactant. Influences of temperature, power ultrasound and reaction time on the morphological properties of $[Hg(L)(I)_2]_n$ (**1**) and $[Hg_2(L^{/})_2(SCN)_2].2H_2O$ (**2**), were studied. These parameters have noticeable influences in the

morphology of the nanoparticles. These systems depicted a decrease in the particles size accompanying an increase of the temperature, and of the power ultrasound as well as a reduction in time reaction. Also, the best conditions for getting a small sized and less agglomerated nanostructure materials for these two mercury coordination supramolecular compounds are temperature, reaction time and the power of ultrasonic irradiation 70 ºC, 60 min and 60 W, respectively.

Supplementary material

Crystallographic data for the structure reported in this paper have been deposited with the Cambridge Crystallographic Data Centre as supplementary publication no. CCDC-1510179 and CCDC-1501127. Copies of the data can be obtained upon application to CCDC, 12 Union Road, Cambridge CB2 1EZ, UK (Fax: +44 1223/336033; e-mail: deposit@ccdc.cam.ac.uk).

Acknowledgement

Support of this investigation by University of Sistan and Baluchestan (USB), Tarbiat Modares University and Institut Català de Nanociència i Nanotecnologia (ICN2) are gratefully acknowledged.

References:

[1] G.-P. Li, G. Liu, Y.-Z. Li, L. Hou, Y.-Y. Wang, Z. Zhu, Uncommon Pyrazoyl-Carboxyl Bifunctional Ligand-Based Microporous Lanthanide Systems: Sorption and Luminescent Sensing Properties, Inorganic chemistry, 55 (2016) 3952-3959.

[2] Z. Hu, B.J. Deibert, J. Li, Luminescent metal–organic frameworks for chemical sensing and explosive detection, Chemical Society Reviews, 43 (2014) 5815-5840.

[3] S. Ghosh, Y. Ida, T. Ishida, A. Ghosh, Linker stoichiometry-controlled stepwise supramolecular growth of a flexible Cu2Tb single molecule magnet from monomer to dimer to one-dimensional chain, Crystal Growth & Design, 14 (2014) 2588-2598.

[4] B. Chen, L. Wang, Y. Xiao, F.R. Fronczek, M. Xue, Y. Cui, G. Qian, A luminescent metal–organic framework with Lewis basic pyridyl sites for the sensing of metal ions, Angewandte Chemie International Edition, 48 (2009) 500-503.

[5] J.-S. Wang, F.-Z. Jin, H.-C. Ma, X.-B. Li, M.-Y. Liu, J.-L. Kan, G.-J. Chen, Y.-B. Dong, Au@ Cu (II)-MOF: Highly Efficient Bifunctional Heterogeneous Catalyst for Successive Oxidation–Condensation Reactions, Inorg. Chem, 55 (2016) 6685-6691.

[6] (a) W.-Y. Gao, C.-Y. Tsai, L. Wojtas, T. Thiounn, C.-C. Lin, S. Ma, Interpenetrating Metal–Metalloporphyrin Framework for Selective CO2 Uptake and Chemical Transformation of CO_2, Inorganic Chemistry, 55 (2016) 7291-7294.

(b) H. Kobayashi, Y. Mitsuka, H. Kitagawa, Metal Nanoparticles Covered with a Metal–Organic Framework: From One-Pot Synthetic Methods to Synergistic Energy Storage and Conversion Functions, Inorganic Chemistry, 55 (2016) 7301-7310.

[7] (a) J. Gu, Y. Cui, X. Liang, J. Wu, D. Lv, A.M. Kirillov, Structurally Distinct Metal–Organic and H-Bonded Networks Derived from 5-(6-Carboxypyridin-3-yl) isophthalic Acid: Coordination and Template Effect of 4, 4′-Bipyridine, Crystal Growth & Design, 16 (2016) 4658-4670.

(b) Y. Wang, S.-S. Meng, P.-X. Lin, Y.-W. Xiao, Q.-Q. Ma, Q. Xie, Y.-Y. Chen, X.-J. Zhao, J. Chen, Solvent-Induced Single Crystal–Single Crystal Transformation of an Interpenetrated Three-Dimensional Copper Triazole Catalytic Framework, Inorganic chemistry, 55 (2016) 4069-4071.

[8] F. Yuan, X. Wang, H.-M. Hu, S.-S. Shen, R. An, G.-L. Xue, Syntheses, structures and luminescent properties of two new zinc coordination polymers based on 4′-(4-aminephenyl)-4, 2′: 6′, 4 ″-terpyridine, Inorganic Chemistry Communications, 48 (2014) 26-29.

[9] D.-M. Chen, J.-Y. Tian, S.-M. Fang, C.-S. Liu, Gas sorption studies on a highly-thermostable microporous Zn (II) coordination polymer constructed from 2D honeycomb layers, Inorganic Chemistry Communications, 66 (2016) 69-72.

[10] A. Galet, V. Niel, M.C. Muñoz, J.A. Real, Synergy between spin crossover and metallophilicity in triple interpenetrated 3D nets with the NbO structure type, Journal of the American Chemical Society, 125 (2003) 14224-14225.

[11] C.-C. Wang, S.-C. Dai, H.-W. Lin, G.-H. Lee, H.-S. Sheu, Y.-H. Lin, H.-L. Tsai, Assembly of metal coordination framework,[M II (C 5 O 5)(dpe)], with a 2D bi-layer architecture: Thermal stability and magnetic properties (M= Mn, Fe, Cd and Co; dpe= 1, 2-bis (4-pyridyl) ethane), Inorganica Chimica Acta, 360 (2007) 4058-4067.

[12] H. Xu, Y. Li, Two new microporous coordination polymers constructed by ladder-like and ribbon-like molecules with cavities, Journal of molecular structure, 693 (2004) 11-15.

[13] J. Luo, M. Hong, R. Wang, R. Cao, L. Han, D. Yuan, Z. Lin, Y. Zhou, A novel bilayer cobalt (II)-organic framework with nanoscale channels accommodating large organic molecules, Inorganic chemistry, 42 (2003) 4486-4488.

[14] K. Barthelet, J. Marrot, D. Riou, G. Férey, A breathing hybrid organic–inorganic solid with very large pores and high magnetic characteristics, Angewandte Chemie, 114 (2002) 291-294.

[15] X.H. Bu, M.L. Tong, H.C. Chang, S. Kitagawa, S.R. Batten, A Neutral 3D Copper Coordination Polymer Showing 1D Open Channels and the First Interpenetrating NbO- Type Network, Angewandte Chemie International Edition, 43 (2004) 192-195.

[16] F. Yuan, L. Zhang, H.-M. Hu, C. Bai, G. Xue, Four new coordination polymers based on carboxyphenyl-substituted dipyrazinylpyridine ligand: Syntheses, structures, magnetic and luminescence properties, Journal of Molecular Structure, 1128 (2017) 385-390.

[17] D.M.S. Paqhaleh, L. Hashemi, V. Amani, A. Morsali, A. Aminjanov, Synthesis of two new nano-structured mercury (ll) complexes with 4-methyl-4H-1, 2, 4-triazole-3-thiol ligand by sonochemical method, Inorganica Chimica Acta, 407 (2013) 1-6.

[18] A. Morsali, M.Y. Masoomi, Structures and properties of mercury (II) coordination polymers, Coordination Chemistry Reviews, 253 (2009) 1882-1905.

[19] T.S.B. Baul, S. Kundu, S. Mitra, H. Höpfl, E.R. Tiekink, A. Linden, The influence of counter ion and ligand methyl substitution on the solid-state structures and photophysical properties of mercury (II) complexes with (E)-N-(pyridin-2-ylmethylidene) arylamines, Dalton Transactions, 42 (2013) 1905-1920.

[20] H.R. Khavasi, A. Azhdari Tehrani, Influence of Halogen Bonding Interaction on Supramolecular Assembly of Coordination Compounds; Head-to-Tail N⋯ X Synthon Repetitivity, Inorganic chemistry, 52 (2013) 2891-2905.

[21] H.R. Khavasi, A.A. Tahrani, The role of secondary bonding on supramolecular assembly of coordination compounds: diversity of coordination modes and supramolecular structures, CrystEngComm, 15 (2013) 5799-5812.

[22] A.A. Tehrani, A. Morsali, M. Kubicki, The role of weak hydrogen and halogen bonding interactions in the assembly of a series of Hg (II) coordination polymers, Dalton Transactions, 44 (2015) 5703-5712.

[23] G.B. Deacon, P.W. Felder, P.C. Junk, K. Müller-Buschbaum, T.J. Ness, C.C. Quitmann, The X-ray crystal structures of [Hg (C 6 F 4 OH-p) 2 OH 2] and [Hg (C 6 H 4 OMe-p)(O 2 CC 6

F 4 OMe-p)]–factors influencing supramolecular Hg–O interactions, Inorganica chimica acta, 358 (2005) 4389-4393.

[24] H. Lee, M. Diaz, C.B. Knobler, M.F. Hawthorne, Octahedral Coordination of an Iodide Ion in an Electrophilic Sandwich, Angewandte Chemie, 112 (2000) 792-794.

[25] W.-T. Chen, M.-S. Wang, X. Liu, G.-C. Guo, J.-S. Huang, Investigations of Group 12 (IIB) Metal Halide/Pseudohalide-Bipy Systems: Syntheses, Structures, Properties, and TDDFT Calculations (Bipy= 2, 2'-bipyridine or 4, 4'-bipyridine), Crystal growth & design, 6 (2006) 2289-2300.

[26] G. Mahmoudi, A. Morsali, A.D. Hunter, M. Zeller, Mercury (II) coordination polymers generated from 1, 4-bis (2 or 3 or 4-pyridyl)-2, 3-diaza-1, 3-butadiene ligands, CrystEngComm, 9 (2007) 704-714.

[27] M.C. Bernini, F. Gándara, M. Iglesias, N. Snejko, E. Gutiérrez- Puebla, E.V. Brusau, G.E. Narda, M. Monge, Reversible Breaking and Forming of Metal–Ligand Coordination Bonds: Temperature- Triggered Single- Crystal to Single- Crystal Transformation in a Metal–Organic Framework, Chemistry–A European Journal, 15 (2009) 4896-4905.

[28] J.H. Bang, K.S. Suslick, Sonochemical synthesis of nanosized hollow hematite, Journal of the American Chemical Society, 129 (2007) 2242-2243.

[29] K. Akhbari, A. Morsali, P. Retailleau, Effect of two sonochemical procedures on achieving to different morphologies of lead (II) coordination polymer nano-structures, Ultrasonics sonochemistry, 20 (2013) 1428-1435.

[30] T. Fujimoto, S.-y. Terauchi, H. Umehara, I. Kojima, W. Henderson, Sonochemical preparation of single-dispersion metal nanoparticles from metal salts, Chemistry of Materials, 13 (2001) 1057-1060.

[31] S. Naveenraj, S. Anandan, A. Kathiravan, R. Renganathan, M. Ashokkumar, The interaction of sonochemically synthesized gold nanoparticles with serum albumins, Journal of pharmaceutical and biomedical analysis, 53 (2010) 804-810.

[32] T. Fujimoto, S.-y. Terauchi, H. Umehara, I. Kojima, W. Henderson, Sonochemical preparation of single-dispersion metal nanoparticles from metal salts, Chemistry of Materials, 13 (2001) 1057-1060.

[33] O. Grinberg, M. Hayun, B. Sredni, A. Gedanken, Characterization and activity of sonochemically-prepared BSA microspheres containing Taxol–an anticancer drug, Ultrasonics sonochemistry, 14 (2007) 661-666.

[34] N.A. Dhas, A. Gedanken, Characterization of sonochemically prepared unsupported and silica-supported nanostructured pentavalent molybdenum oxide, The Journal of Physical Chemistry B, 101 (1997) 9495-9503.

[35] W.-L. Guo, Z.-X. Yang, X.-K. Wang, Sonochemical deposition and characterization of nanophasic TiO_2 on silica particles, Materials Research Innovations, 10 (2006) 63-68.

[36] M. Ashokkumar, F. Grieser, Ultrasound assisted chemical processes, Reviews in Chemical Engineering, 15 (1999) 41-83.

[37] S. Zhu, H. Zhou, M. Hibino, I. Honma, M. Ichihara, Synthesis of MnO_2 nanoparticles confined in ordered mesoporous carbon using a sonochemical method, Advanced Functional Materials, 15 (2005) 381-386.

[38] M. Bradley, M. Ashokkumar, F. Grieser, Sonochemical production of fluorescent and phosphorescent latex particles, Journal of the American Chemical Society, 125 (2003) 525-529.

[39] L.A. Crum, T.J. Mason, J.L. Reisse, K.S. Suslick, Sonochemistry and sonoluminescence, Springer Science & Business Media, 2013.

[40] H. Weller, Quantized semiconductor particles: a novel state of matter for materials science, Advanced Materials, 5 (1993) 88-95.

[41] H. Bar, D.K. Bhui, G.P. Sahoo, P. Sarkar, S. Pyne, A. Misra, Green synthesis of silver nanoparticles using seed extract of Jatropha curcas, Colloids and Surfaces A: Physicochemical and Engineering Aspects, 348 (2009) 212-216.

[42] M.J.S. Fard, P. Hayati, A. Firoozadeh, J. Janczak, Ultrasonic synthesis of two new zinc (II) bipyridine coordination polymers: New precursors for preparation of zinc (II) oxide nano-particles, Ultrasonics Sonochemistry, 35 (2017) 502-513.

[43] E. Kemnitz, U. Groß, S. Rüdiger, C.S. Shekar, Amorphous metal fluorides with extraordinary high surface areas, Angewandte Chemie International Edition, 42 (2003) 4251-4254.

[44] A. Carne, C. Carbonell, I. Imaz, D. Maspoch, Nanoscale metal–organic materials, Chemical Society Reviews, 40 (2011) 291-305.

[45] W. Lin, W.J. Rieter, K.M. Taylor, Modular synthesis of functional nanoscale coordination polymers, Angewandte Chemie International Edition, 48 (2009) 650-658.

[46] A.M. Spokoyny, D. Kim, A. Sumrein, C.A. Mirkin, Infinite coordination polymer nano-and microparticle structures, Chemical Society Reviews, 38 (2009) 1218-1227.

[47] A.L. Garay, A. Pichon, S.L. James, Solvent-free synthesis of metal complexes, Chemical Society Reviews, 36 (2007) 846-855.

[48] M.Y. Masoomi, A. Morsali, Morphological study and potential applications of nano metal–organic coordination polymers, RSC Advances, 3 (2013) 19191-19218.

[49] Y. Hanifehpour, V. Safarifard, A. Morsali, B. Mirtamizdoust, S.W. Joo, Sonochemical syntheses of two new flower-like nano-scale high coordinated lead (II) supramolecular coordination polymers, Ultrasonics sonochemistry, 23 (2015) 282-288.

[50] P. Hayati, A.R. Rezvani, A. Morsali, P. Retailleau, S. García-Granda, Influences of temperature, power ultrasound and reaction time on the morphological properties of two new mercury (II) coordination supramolecular compounds, Ultrasonics Sonochemistry, 34 (2017) 968-977.

[51] P. Hayati, A.R. Rezvani, A. Morsali, P. Retailleau, Ultrasound irradiation effect on morphology and size of two new potassium coordination supramolecule compounds, Ultrasonics Sonochemistry, 34 (2017) 195-205.

[52] P. Hayati, A. Rezvani, A. Morsali, P. Retailleau, R. Centore, Survey of temperature, reaction time and ultrasound irradiation power on sonochemical synthesis of two new

nanostructured lead (II) coordination supramolecule compounds, Ultrasonics Sonochemistry, (2016). [53] Rigaku (2014) CrystalClear-SM expert 2.1b43 The Woodlands, Texas, USA, and Rigaku Corporation, Tokyo, Japan.

[54] Sheldrick, G. M. (2015). Acta Cryst. A71, 3-8.

[55] Spek, A. L. (2009). Acta Cryst. D65, 148–155.

[56] SADABS, Bruker-Nonius, Delft, The Netherlands, 2002.

[57] A. Altomare, M. C. Burla, M. Camalli, G. L. Cascarano, C. Giacovazzo, A. Guagliardi, G. G. Moliterni, G. Polidori, R. Spagna, J. Appl. Crystallogr. 32 (1999) 115-119.

[58] G. M. Sheldrick, Acta Crystallogr. A64 (2008) 112-122.

[59] L. J. Farrugia, J. Appl. Crystallogr. 45 (2012) 849-854.

[60] Mercury 1.4.1, Copyright Cambridge Crystallographic Data Centre, 12 Union Road, Cambridge, CB2 1EZ, UK, 2001–2005.

[61] V.A. Blatov, A.P. Shevchenko, D.M. Proserpio, Applied topological analysis of crystal structures with the program package ToposPro, Crystal Growth & Design, 14 (2014) 3576-3586. http://topospro.com.

[62] A.R. Abbasi, A. Morsali, Syntheses and characterization of AgI nano-structures by ultrasonic method: different morphologies under different conditions, Ultrasonics sonochemistry, 17 (2010) 572-578.

[63] A.R. Abbasi, A. Morsali, Formation of silver iodide nanoparticles on silk fiber by means of ultrasonic irradiation, Ultrasonics sonochemistry, 17 (2010) 704-710.

[64] A.R. Abbasi, A. Morsali, Influence of solvents on the morphological properties of AgBr nano-structures prepared using ultrasound irradiation, Ultrasonics sonochemistry, 19 (2012) 540-545.

[65] Y. Noori, K. Akhbari, A. Phuruangrat, F. Costantino, Studies the effects of ultrasonic irradiation and dielectric constants of solvents on formation of lead (II) supramolecular polymer; new precursors for synthesis of lead (II) oxide nanoparticles, Ultrasonics Sonochemistry, 35 (2017) 36-44.

[66] E. Mirzadeh, K. Akhbari, A. Phuruangrat, F. Costantino, A survey on the effects of ultrasonic irradiation, reaction time and concentration of initial reagents on formation of kinetically or thermodynamically stable copper (I) metal-organic nanomaterials, Ultrasonics Sonochemistry, (2016).

[67] F.S. Shirazi, K. Akhbari, Sonochemical procedures; the main synthetic method for synthesis of coinage metal ion supramolecular polymer nano structures, Ultrasonics sonochemistry, 31 (2016) 51-61.

Table 1. Crystal data and structures refinement for $[Hg(L)(I)_2]_n$ **(1)** and $[Hg_2(L)_2(SCN)_2].2H_2O$ (**2**)

Empirical formula	$C_6 H_8 Hg I_2 N_2$	$0.4(C_{16}H_8Hg_2N_4O_8S_2)\cdot 0.8\ H_2O$
Formula weight	562.53	354.24 g/mol
Temperature	203(2) K	293(2) K
Wavelength	0.71075 Å	0.71073Å
Crystal system	Monoclinic	Monoclinic
Space group	P 21/c	$P2_1/c$
Unit cell dimensions	a = 4.3480(2)Å, α=90.000 °	a = 7.0679(2) Å, α =90°
	b = 12.0700(9)Å, β = 91.500(3)°	b =17.9631(4)Å, β=116.336(4)
	c = 20.3618(14)Å,γ=90.000 °	c =20.1454(7)Å, γ =90°
Volume	1068.23 (12)$Å^3$	2292.23 (14) $Å^3$
Z	4	10
Density(calculated)	3.50853 g/cm^3	2.566 g/cm^3
Absorption coefficient	22.135Mg/m^3	13.58 Mg/m^3
F(0 0 0)	976.0	1632
Theta range for data collection	2.00 to 29.08°	4.1 to 31.3°
Reflections collected	3864	26544
μ	20.14 mm^{-1}	13.621mm^{-1}
Index ranges	$-4 \le h \le 6$	$-9 \le h \le 10$
	$-16 \le k \le 16$	$-24 \le k \le 26$
	$-27 \le l \le 27$	$-29 \le l \le 28$
h, k, l (max)	6, 16, 27	9, 27, 16
$(\sin \theta/\lambda)max$	0.698 $Å^{-1}$	0.734 $Å^{-1}$
Theta(max)	26.8°	31.3 °
Radiation type	Mo Kα	Mo Kα
Refinement method	Full– matrix least– squares on F^2	Full– matrix least–squares on F^2
Goodness– of – fit– on F^2	1.080	1.054
Refinement	$R[F^2 > 2\sigma(F^2)]=0.56$	$R[F2 > 2\sigma(F2)]= 0.031$
	$wR(F^2)= 0.136$	wR(F2)= 0.078
	S=1.08	S= 1.05
Extinction coefficient	n/a	0.00081(9)
Largest diff. peak and hole	3.40, −3.00 e $Å^{-3}$	2.44 and -1.61eA^{-3}
CCDC no.	1510179	1501127

Table 2. Selected bond lengths/ Aº for compound $[Hg_2(L)(I)_2]_n$

Hg(1)—N(1)	2.318(12)	N(1)—C(1)	1.334(18)
Hg(1)—I(2)	2.6569(11)	N(1)—C(5)	1.389(17)
Hg(1)—I(1)^{i}	2.7370(11)	N(2)—C(5)	1.385(18)
Hg(1)—I(1)	2.9986(11)	N(2)—H(2)A	0.89(2)
I(1)—Hg(1)^{ii}	2.7371(11)	N(2)—H(2)B	0.88(2)
C(2)—C(1)	1.37(2)	C(1)—H(1)	0.9400
C(2)—C(3)	1.43(2)	C(6)—C(3)	1.48(2)
C(2)—H(2)	0.9400	C(6)—H(6)A	0.9700

Symmetry transformations used to generate equivalent atoms:

(i) -1+x, y, z; (ii) 1+x, y, z.

Table 3. Selected bond lengths/ Aº for compound $[Hg_2(L)_2(SCN)_2].2H_2O$

Hg1A—S1B	2.3776(11)	N1A—C7A	1.327(5)
Hg1A—O4A	2.528(3)	N1B—C7B	1.338(5)
Hg1A—O1A	2.465(3)	N1B—C3B	1.350(5)
Hg1A—N2A	2.412(4)	C1A—C7A	1.511(6)
Hg1A—N1A	2.217(3)	C4B—H4B	0.9300
Hg1B—S1A	2.3755(11)	C4B—C3B	1.374(6)
Hg1B—O1B	2.471(3)	C4B—C5B	1.387(6)
Hg1B—O4B	2.521(3)	C1B—C7B	1.492(6)
Hg1B—N2B	2.419(4)	C4A—H4A	0.9300
Hg1B—N1B	2.216(3)	C4A—C3A	1.379(6)

Table 4. The influence of temperature, reaction time and sonication power on the size of compound 1 and 2 particles.

Compound 2 samples	T (°C)[a]	T (min)[b]	Sonication (input power) (W)	Size[c] (nm)
1 - 1	50	60	0	820
1 - 2	50	60	60	122
1 - 3	50	30	60	108
1 - 4	70	60	60	85
Compound 3 samples	T(°C)[a]	T(min)[b]	Sonication (input power) (W)	Size[c] (nm)
2 - 1	50	60	0	530
2 - 2	50	60	60	78
2 - 3	50	30	60	64
2 - 4	70	60	60	47

[a] Reaction temperature

[b] Reaction time

[c] Average diameter (nm)

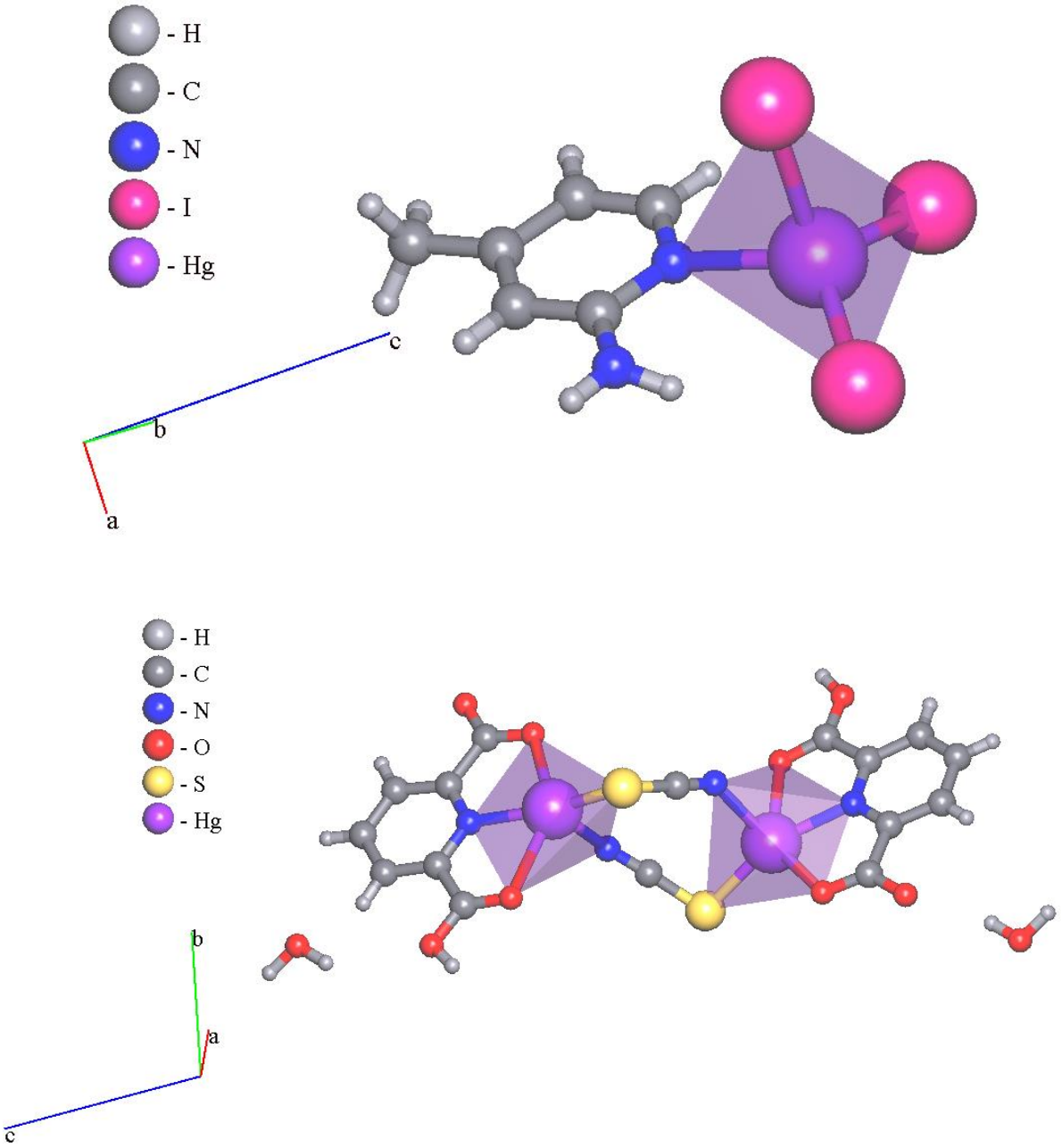

Figure. 1. The coordination environment of Hg^{+2} cation environment in compound and in compound 1(up), compound 2 (down).

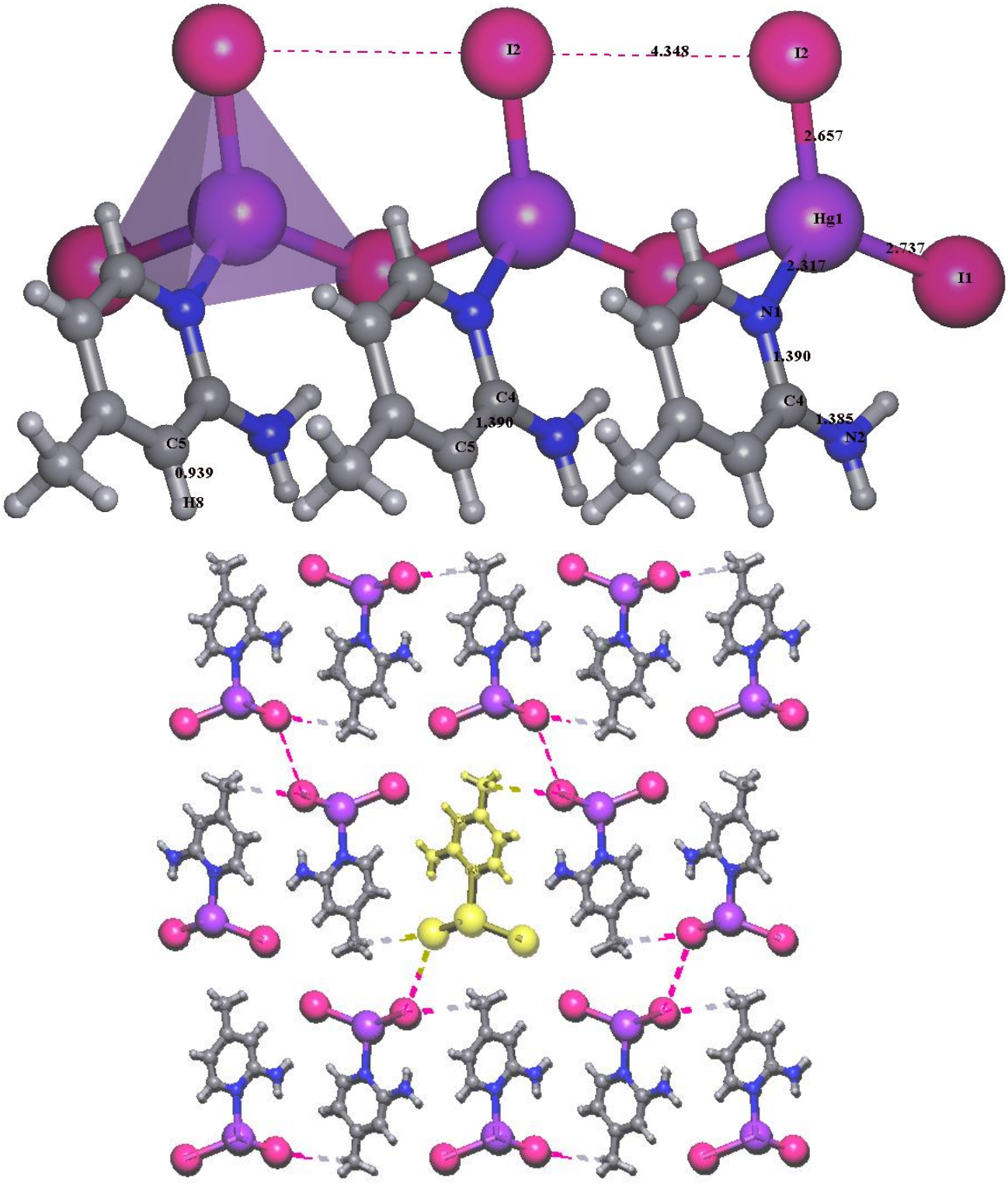

Fig. 2. Eight chains surrounding the central one. Distance of bounds in 1 (up). Dashed lines represent van-der-waales bonded (down).

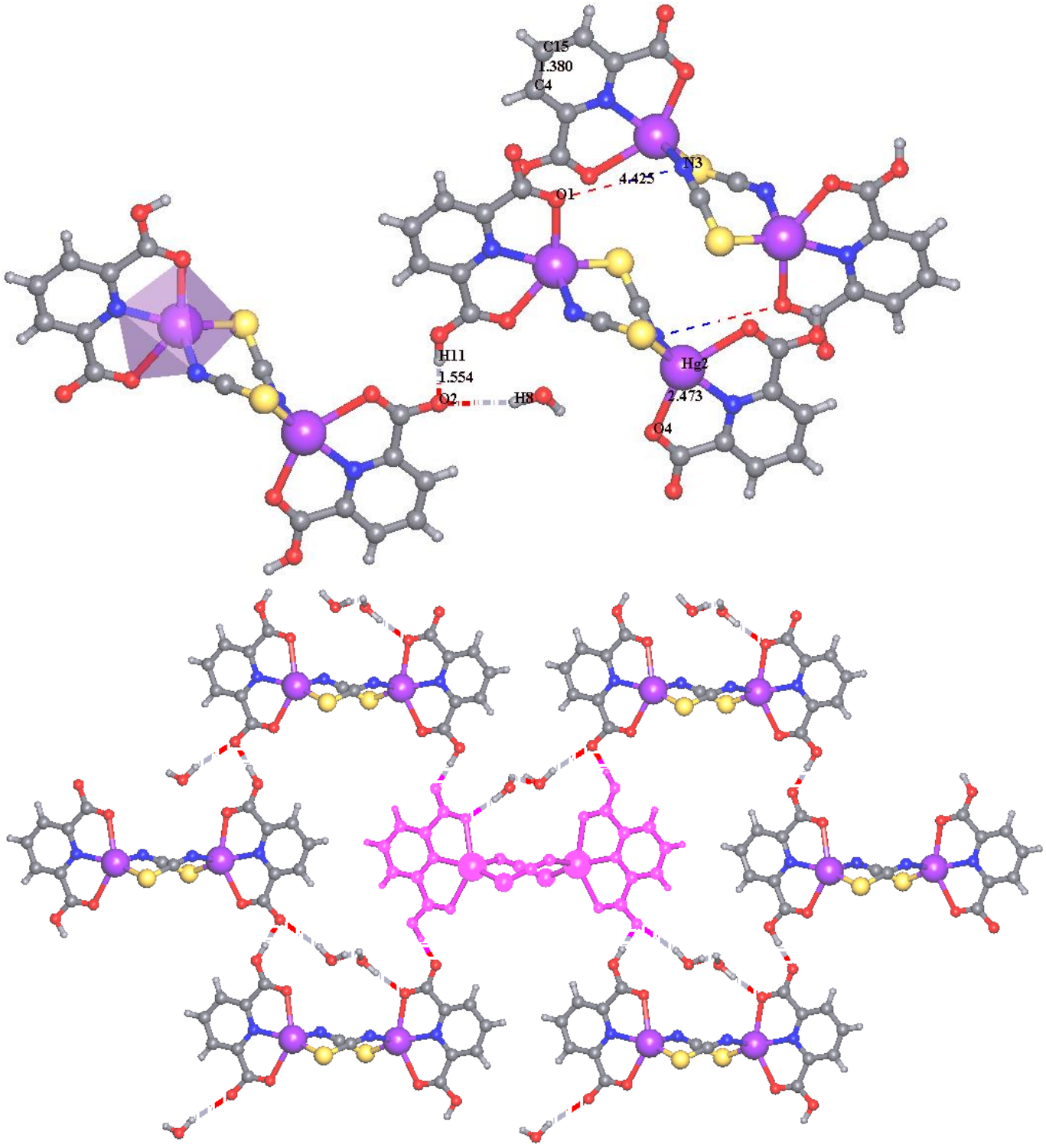

Fig. 3. Eight chains surrounding the central one. Distance of bounds in 2 (up). Dashed lines represent H-bonds (down).

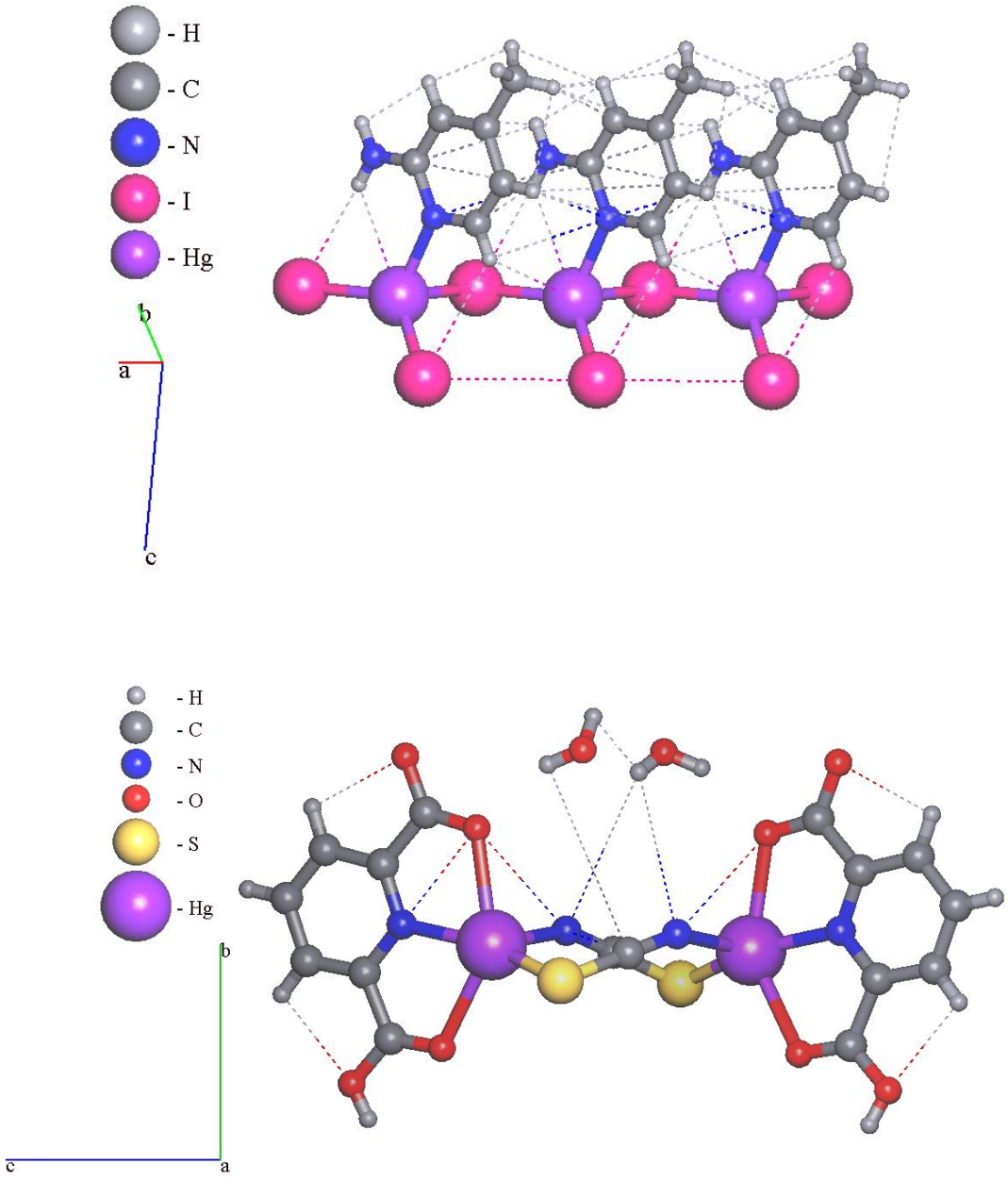

Fig. 4. Weak interaction in asymmetric units compound 1(up), compound 2 (down).

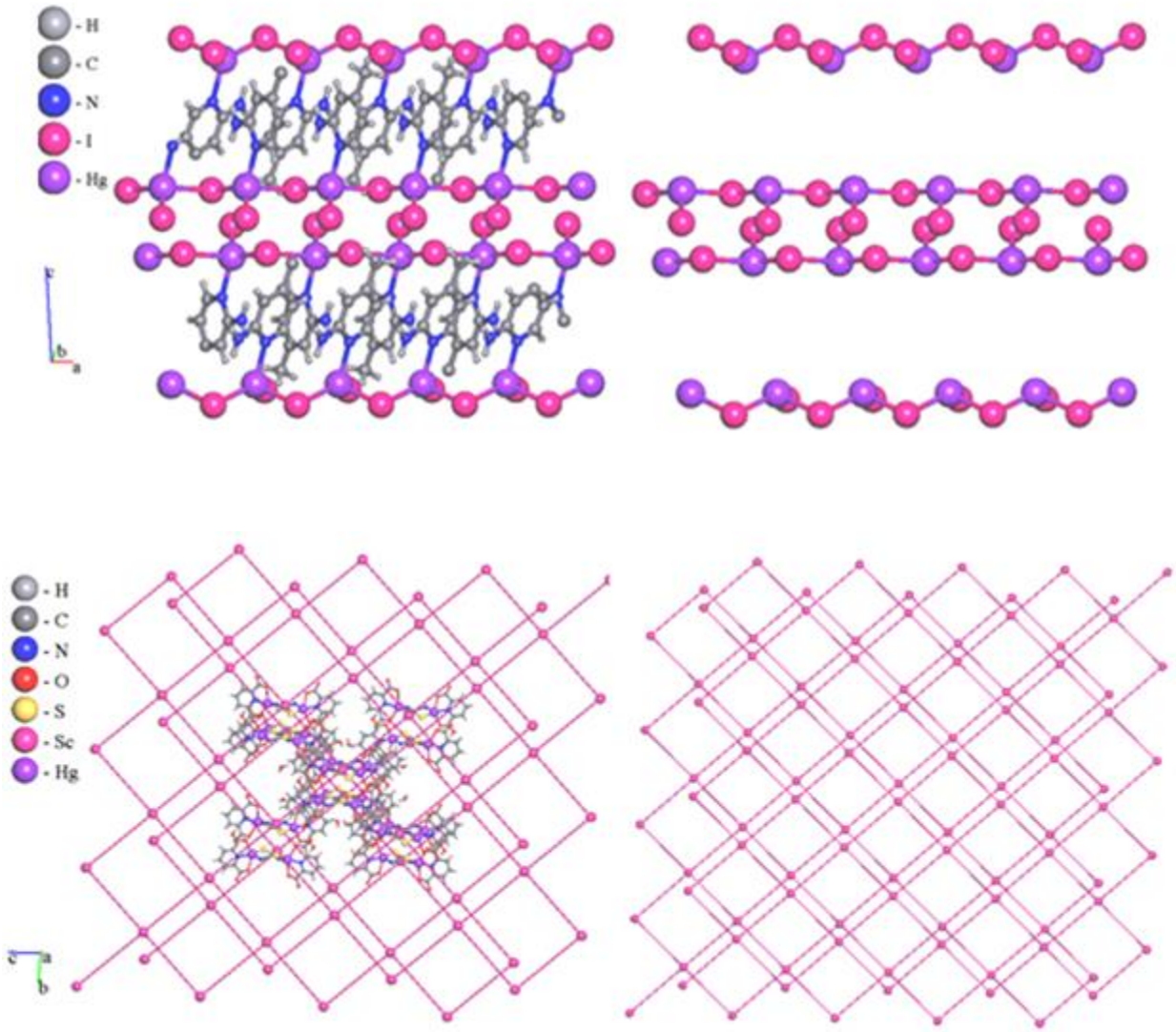

Fig. 5. Topological representation of coordination networks in compounds 1 (up), 2 (down).

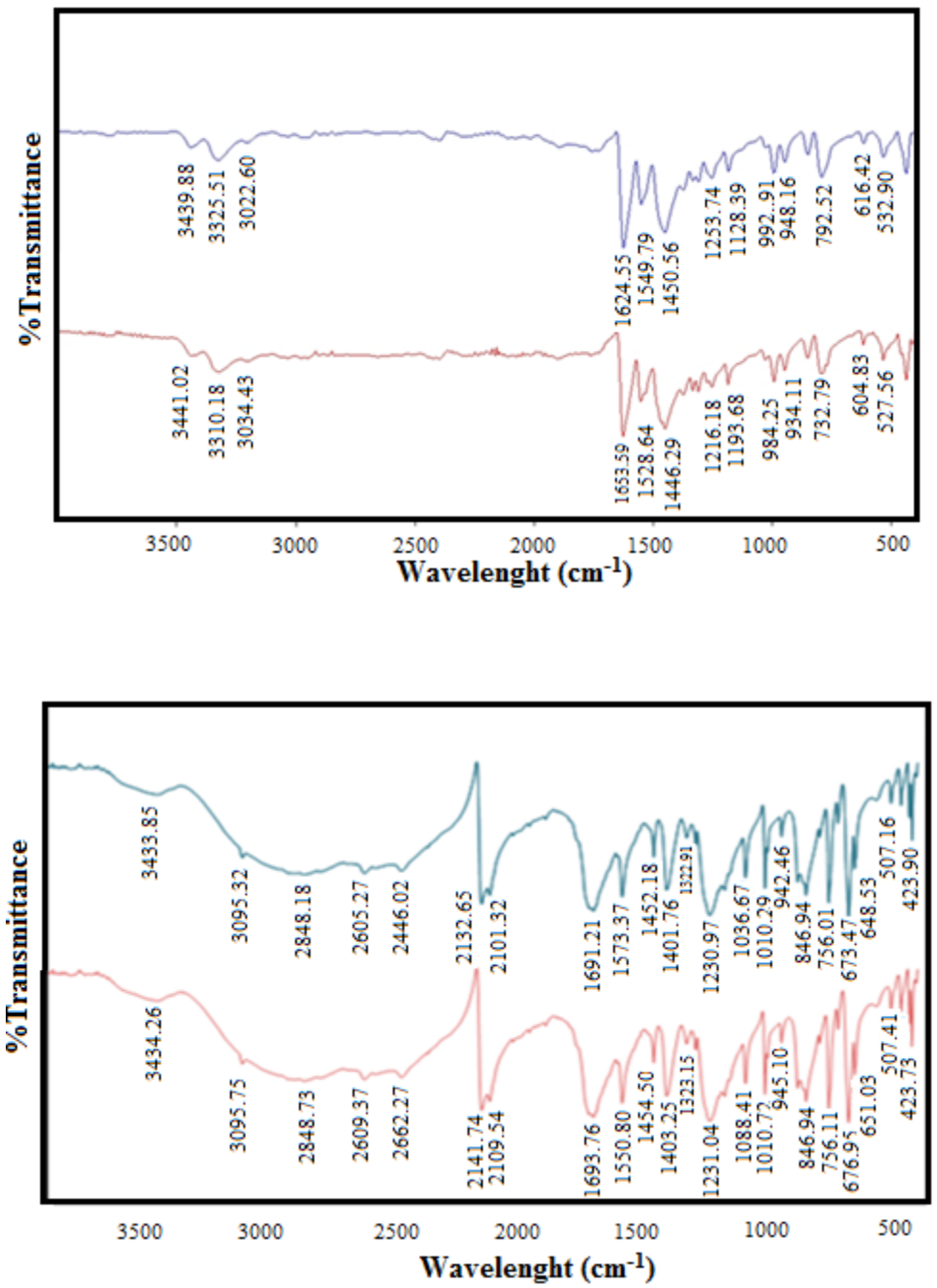

Figure. 6. The IR spectra of (blue line) bulk materials as synthesized of compound 1 and (red line) nano-sized compound 1 prepared by sonochemical method (up), (blue line) bulk materials as synthesized of compound 2 and (red line) nano-sized compound 2 prepared by sonochemical method (down).

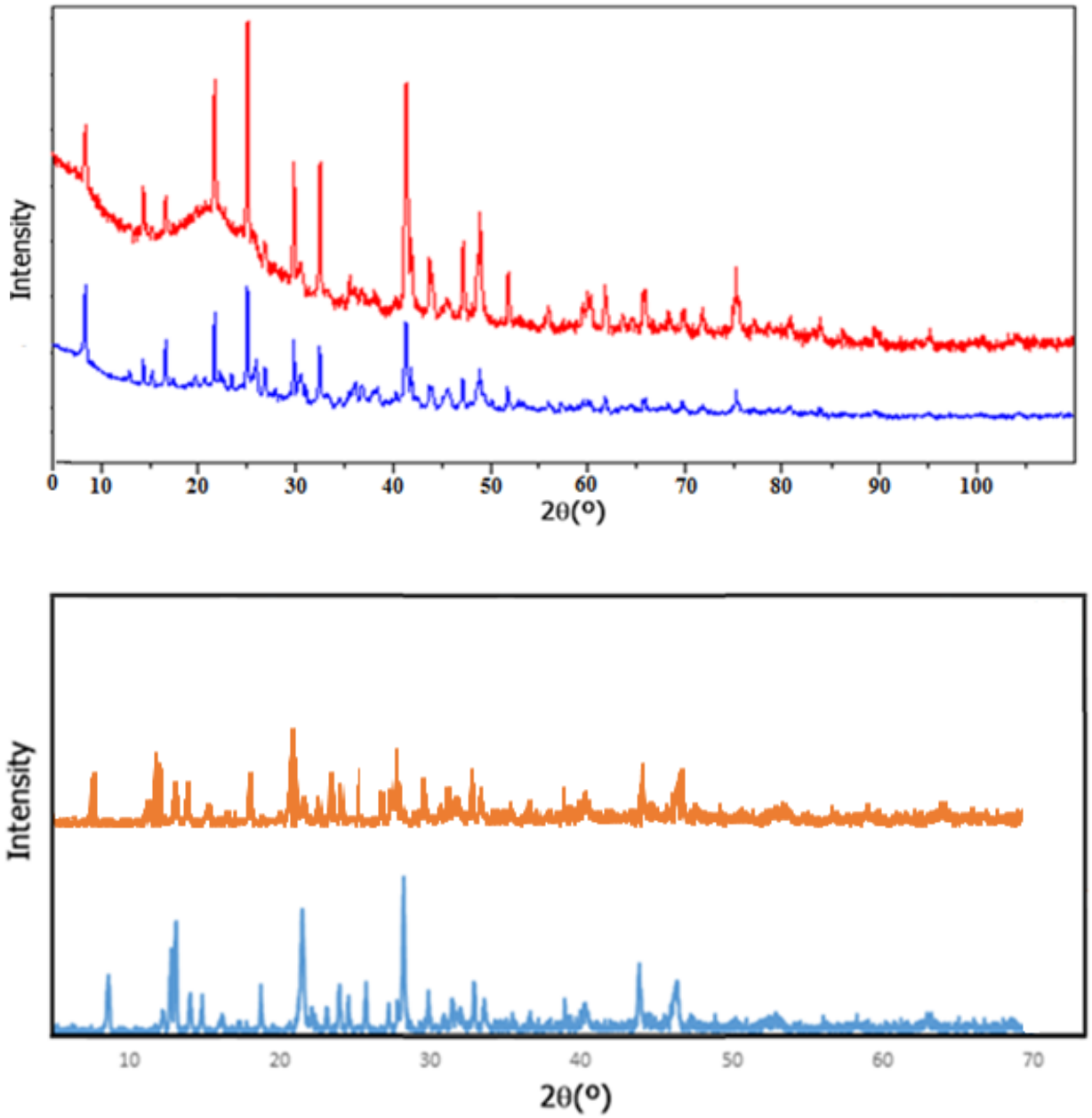

Figure. 7. The PXRD patterns of (blue line) nano-sized 1 obtained by ultrasonication, (red line) simulated from single crystal X-ray data of 1 (up), (brown line) nano-sized 2obtained by ultrasonication, (blue line) simulated from single crystal X-ray data of 2 (down).

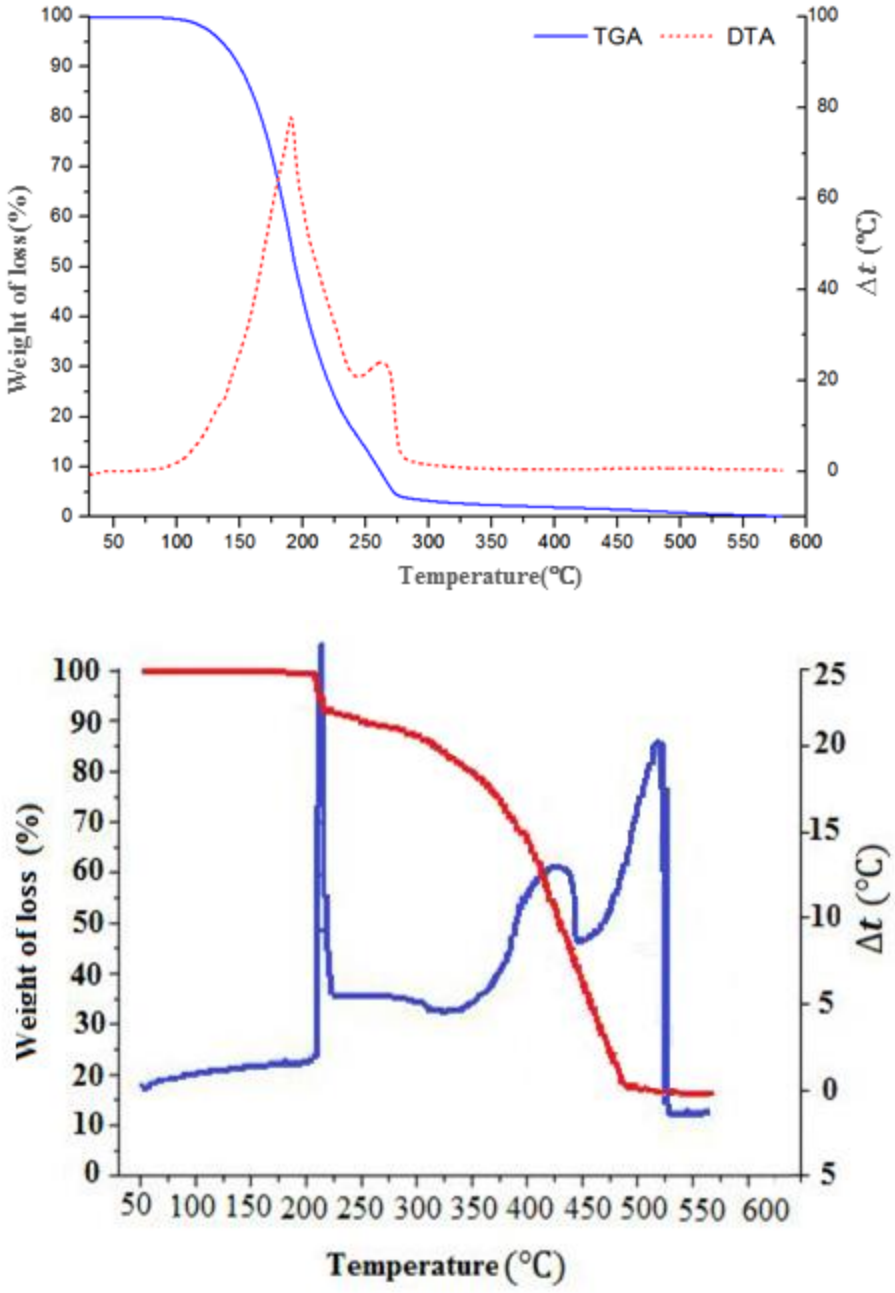

Figure. 8. Thermal behavior of compound 1 (up), 2 (down).

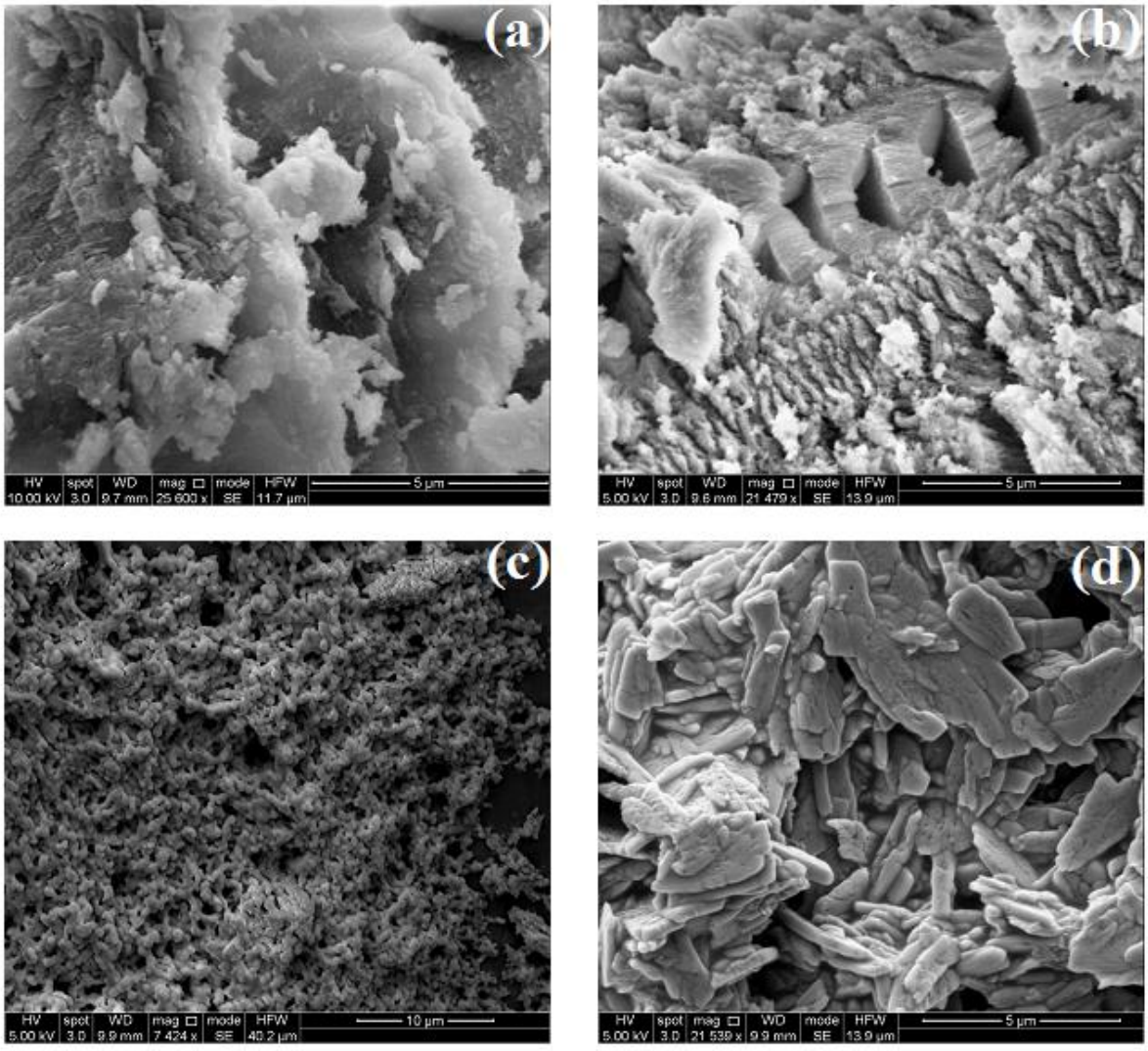

Figure. 9. SEM image of nanostructure 1, (a) without sonochemical reaction, (b) by sonochemical reaction with sonochemical temperature of 50°C, time of 60 min and power of 60W, (c) by sonochemical reaction with sonochemical temperature of 50°C, time of 30 min and power of 60W, (d) by sonochemical reaction with sonochemical temperature of 70°C, time of 60 min and power of 60W.

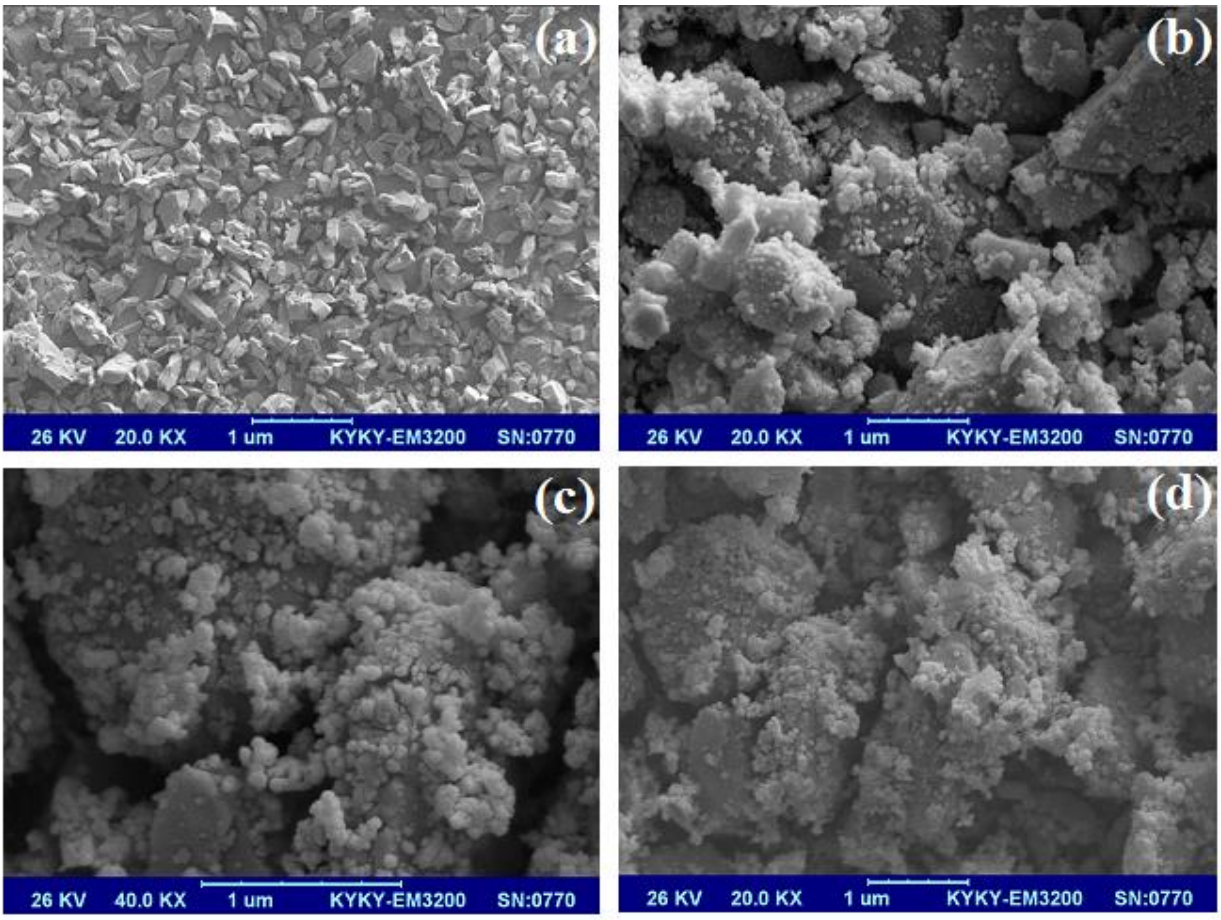

Figure .10. SEM image of nanostructure 2, (a) without sonochemical reaction, (b) by sonochemical reaction with sonochemical temperature of 50°C, time of 60 min and power of 60W, (c) by sonochemical reaction with sonochemical temperature of 50°C, time of 30 min and power of 60W, (d) by sonochemical reaction with sonochemical temperature of 70°C, time of 60 min and power of 60W.